JAERI-M
7917

ASCOT-I: A COMPUTER PROGRAM FOR ANALYZING THE THERMO-HYDRAULIC BEHAVIOR IN A PWR CORE DURING A LOCA

September 1978

Kensuke KOBAYASHI and Kazuo SATO

日本原子力研究所
Japan Atomic Energy Research Institute

この報告書は，日本原子力研究所が JAERI-M レポートとして，不定期に刊行している研究報告書です．入手，複製などのお問合わせは，日本原子力研究所技術情報部（茨城県那珂郡東海村）あて，お申しこしください．

JAERI-M reports, issued irregularly, describe the results of research works carried out in JAERI. Inquiries about the availability of reports and their reproduction should be addressed to Division of Technical Information, Japan Atomic Energy Research Institute, Tokai-mura, Naka-gun, Ibaraki-ken, Japan.

JAERI-M 7917

ASCOT-1: A Computer Program for Analyzing the Thermo-Hydraulic Behavior in a PWR Core during a LOCA

Kensuke KOBAYASHI and Kazuo SATO
Division of Reactor Safety Evaluation,
Tokai Research Establishment, JAERI

(Received September 21, 1978)

A digital computer code ASCOT-1 has been developed to analyze the thermo-hydraulic behavior in a PWR core during a loss-of-coolant accident. The core is assumed to be axi-symmetric two-dimensional and the conservation laws are solved by the method of characteristics. For the temperature response of representative fuels of the concentric annular subregions into which the core is divided, the heat conduction equations are solved by the explicit method with the averaged flow conditions decided above.

The boundary conditions at the upper and lower plenum are given as inputs. The program is of an adjustable dimension so there are no restrictions to the numbers of meshes. ASCOT-1 is written in FORTRAN-IV for FACOM230-75.

Keywords: LOCA, PWR Core, Computer Code, Thermo-Hydraulic Behavior, Axi-Symmetric Two-Dimensional Calculation, Method of Characteristics, Conservation Laws, Fuel Temperature, Heat Conduction Equation, Explicit method

JAERI－M 7917

ＬＯＣＡ時の加圧型炉炉心における熱水力学的挙動を解析するプログラム：ＡＳＣＯＴ－１

日本原子力研究所東海研究所安全解析部
小林　健介・佐藤　一男

（１９７８年９月２１日受理）

冷却材喪失事故時の加圧水型炉炉心における熱水力学的挙動を解析するプログラムＡＳＣＯＴ－１を開発した。炉心を軸対称２次元と仮定し，保存則を特性曲面法によって解く。炉心を分割した同心円環状部分領域の代表燃料棒の温度応答にたいしては，平均化された流動条件を用いて熱伝導方程式を陽的解法によって求める。

上部プレナムおよび下部プレナムにおける境界条件は入力として与えられる。整合寸法を用いているため格子点数の制限はない。ＡＳＣＯＴ－１はＦＡＣＯＭ２３０－７５用のＦＯＲＴＲＡＮ－Ⅳで書かれている。

CONTENTS

1. Introduction 1

2. Fundamental equations 3

2.1 Two-dimensional hydraulics of core flow 3

2.2 Heat condition inside representative fuel rods 5

2.3 Heat transfer coefficients 9

3. Method of computation 10

3.1 Two-dimensional hydraulics of core flow 10

3.2 Heat conduction inside representative fuel rods 13

3.3 Metal-water reaction 18

3.4 Clad swelling and rupture model 20

3.5 Flow resistance 21

3.6 Boundary conditions 23

4. Comparison with an analytical solution 26

Acknowledgement 27

Reference 28

Appendix A Nomenclature 31

Appendix B Code description 34

B.1 Input description 34

B.2 Output description 48

Appendix C Steam table for ASCOT-1 49

Appendix D Fuel rods material properties built in ASCOT-1 50

目　　次

1. はじめに …… 1
2. 基礎方程式 …… 3
2.1 炉心流動の２次元水力学 …… 3
2.2 代表燃料棒内熱伝導 …… 5
2.3 熱伝達係数 …… 9
3. 計算方法 …… 10
3.1 炉心流動の２次元水力学 …… 10
3.2 代表燃料棒内熱伝導 …… 13
3.3 金属－水反応 …… 18
3.4 被覆管のふくれと破裂のモデル …… 20
3.5 流動抵抗 …… 21
3.6 境界条件 …… 23
4. 解析解との比較 …… 26
謝　辞 …… 27
参考文献 …… 28
付録 A　記号表 …… 31
付録 B　コードの記述 …… 34
付録 B. 1　入力の記述 …… 34
付録 B. 2　出力の記述 …… 48
付録 C　ＡＳＣＯＴ－１の蒸気表 …… 49
付録 D　ＡＳＣＯＴ－１に組みこまれている燃料棒材料物性値 …… 50

1. Introduction

A digital computer code ASCOT-1, written entirely in FORTRAN-IV for FACOM230-75, has been developed to study the thermo-hydraulic behavior of a reactor core in PWR's during the blowdown phase of loss-of-coolant accidents (LOCA). ASCOT-1 code forms part of the code system for PWR ECCS evaluation being developed by Japan Atomic Energy Research Institute. ASCOT-1 code analyzes the detailed coolant behavior and the temperature response of representative fuels in the core with the boundary conditions given by a loop code such as ALARM-P1 code.[1]

For the coolant behavior, the core region is treated as continuous but non-isotropic two-dimensional flow field. This is required by the fact that the core has no channel boxes to restrict possible cross-flow due to clad swelling, power distribution and so on. The core is assumed to be axi-symmetrical, and a number of mesh points are distributed on the z-r plane. The effects of the complicated flow boundary formed by fuel rods and other structures which may be deformed during blowdown are represented by equivalent flow resistances for z or r directions. This model, developed by V.J. Esposito et al., is called a macro-micro approach.[2] The heat input from the fuels to the coolant is also defined at each mesh point. The method of characteristics is extended and applied to solve the conservation laws in the axi-symmetric two-dimensional flow field.[3]

For the temperature response of representative fuels, the core region is divided into several concentric annular subregions. In each subregion, a representative fuel rod is selected and the coolant flow conditions are averaged with respect to r and z, thus giving the averaged flow conditions as functions of time for each subregion. The heat conduction equation for the representative fuel rod is solved with the averaged flow conditions. The heat transfered to the coolant from the representative fuel rod is then

multiplied by the number of the fuel rods in the subregion and distributed uniformly to the mesh points belonging to the subregion.

In the ASCOT-1 code, two sets of heat transfer models are incorporated, one having four heat transfer modes; subcooled convective cooling, nucleate boiling, stable film boiling and superheated steam convective cooling and the other having nine heat transfer modes; subcooled forced convection, nucleate boiling, forced convection vaporization, transition boiling, stable film boiling, pool film boiling, transition film boiling, superheated vapor forced convection, and low pressure flow film boiling.

In this report, fundamental equations, method of computations and boundary conditions are described. Also are given in Appendices the property values, and the outline of the program.

2. Fundamental Equations

2.1 Two-dimensional Hydraulics of Core Flow

The laws of conservation of mass, momentum and energy are numerically solved in ASCOT-1 for core flow under the following assumptions:

(1) axi-symmetric two-dimensional

(2) homogeneous flow, and

(3) thermal equilibrium.

Then, the laws of conservation of mass, momentum and energy can be described, as follows:

Mass

$$\frac{\partial \rho}{\partial t} + \frac{1}{r} \frac{\partial}{\partial r}(\rho v_r) + \frac{\partial}{\partial z}(\rho v_z) = 0 \tag{1}$$

Momentum

$$\rho\left(\frac{\partial v_r}{\partial t} + v_r \frac{\partial v_r}{\partial r} + v_z \frac{\partial v_r}{\partial z}\right) = -\frac{\partial p}{\partial r} - F_r \tag{2}$$

$$\rho\left(\frac{\partial v_z}{\partial t} + v_r \frac{\partial v_z}{\partial r} + v_z \frac{\partial v_z}{\partial z}\right) = -\frac{\partial p}{\partial z} - F_z - \rho g_z \tag{3}$$

Energy

$$-c^2\left(\frac{\partial \rho}{\partial t} + v_r \frac{\partial \rho}{\partial r} + v_z \frac{\partial \rho}{\partial z}\right) + \frac{\partial p}{\partial t} + v_r \frac{\partial p}{\partial r} + v_z \frac{\partial p}{\partial z}$$

$$= -\frac{(Q''' + Fe)c^2}{\rho h_\rho} \tag{4}$$

where these equations are based on the macro-micro approach.[2] The core region is treated as a continuous flow field and the effects of the complicated flow boundary formed by fuel rods and other structures are represented by effective flow resistances of the form

$$F_r = - f_r \frac{\rho |v_r| v_r}{2D_e}$$

$$F_z = - f_z \frac{\rho |v_z| v_z}{2D_e}$$

where f_r depends on a Reynolds number based on the v_r component of velocity and f_z on the v_z component of velocity.

The F_e represents the irreversible energy terms due to frictional losses. Q''' stands for the term of heating rate per unit volume. Equations (1) through (4) is a set of quasi-linear hyperbolic partial differential equations hence the method of characteristics is applicable to the equations. A set of bicharacteristic curves and compatibility equations equivalent to them is obtained by using the method of characteristics as follows,

$$\frac{dr}{dt} = v_r , \qquad \frac{dz}{dt} = v_z \tag{5}$$

$$-c^2 \frac{D_p \rho}{Dt} + \frac{D_p p}{Dt} = - \frac{(Q''' + F_e)c^2}{\rho h_\rho} \tag{6}$$

$$\rho c \cos\theta \frac{D_\theta v_r}{Dt} + \rho c \sin\theta \frac{D_\theta v_z}{Dt} + \frac{D_\theta p}{Dt} + \rho c^2 [\sin\theta \frac{D_1 v_r}{Dt} - \cos\theta \frac{D_1 v_z}{Dt}]$$

$$= - c^2 \frac{\rho v_r}{r} - c \cos\theta F_r - c \sin\theta (F_z + \rho g_z) - \frac{(Q''' + F_e)c^2}{\rho h_\rho} \tag{7}$$

where $$\frac{D_\theta}{D_t} = \frac{\partial}{\partial t} + (v_r + c \cos\theta) \frac{\partial}{\partial r} + (v_z + c \sin\theta) \frac{\partial}{\partial z} \tag{8}$$

and $$\frac{D_1}{Dt} = \sin\theta \frac{\partial}{\partial r} - \cos\theta \frac{\partial}{\partial z} \tag{9}$$

2.2 Heat Conduction inside Representative Fuel Rod

The core region is divided into several concentric annular subregions. In each subregion, a representative fuel rod is selected, and the heat conduction equations inside the representative fuel rod is solved with the averaged flow conditions and the heat transfer correlations. Only radial heat conduction is assumed to occur inside the fuel rod. Thus the heat conduction equation inside the fuel rod is given in the (i,j)-th subregion as follows,

$$\rho c_p \frac{\partial T}{\partial t} = \frac{1}{r} \frac{\partial}{\partial r} \left(kr \frac{\partial T}{\partial r} \right) + \dot{Q}(t,r,i,j) \tag{10}$$

where ρ, c_p and k represent density, heat capacity and thermal conductivity, respectively, and Q(t,r,i,j) stands for heat generation due to fission, fission product decay and decay of actinides in the (i,j)-th subregion.

The property values of pellet and clad, such as density, heat capacity and thermal conductivity, will be described in Appendix B and D.

The linear heat rate is assumed to be space-time separable. Thus this is given as follows:

$$\dot{Q}(t,r,i,j) = \dot{Q}^{CORE}(t) \quad \Phi(r,i,j) \tag{11}$$

$$\text{where} \quad \dot{Q}^{CORE}(t) = \dot{Q}^{CORE}(o) \left[S^{FP}(t) + S^{ACT}(t) + S^{FIS}(t) \right] \tag{12}$$

$S^{FP}(t)$: the ratio of heat rate from fission product decay at a time t to total heat rate in core at t=o, $\dot{Q}^{CORE}(o)$,

$S^{ACT}(t)$: the ratio of heat rate from decay of actinides to $\dot{Q}^{CORE}(o)$,

$S^{FIS}(t)$: the ratio of heat rate from fission heat to $\dot{Q}^{CORE}(o)$,

$\Phi(r,i,j)$: space-distribution function of heat generation.

The decay heat of fission products is calculated with the Shure's correlation[4] for infinite operating time and the modification factor given as input data. Thus

$$S^{FP}(t) = \alpha^{FP} \cdot A\, t^{-a} \tag{13}$$

where α^{FP} stands for the modification factor and A and a represent coefficients modified in SCORCH-B2 code[5] in order to make Eq.(13) continuous as given in Table 1. The ratio of heat generation rate from the radioactive decay of actinides at a time t to the total heat rate in core at t=o is calculated with the following equation (14) by assuming infinite operating time and only decay of ^{239}U and ^{239}Np. Thus

$$S^{ACT}(t) = S^{ACT}(o)(0.512\ e^{-4.91\times10^{-4}t} + 0.488) \tag{14}$$

where $S^{ACT}(o)$ represents the ratio of heat generation rate from the radioactive decay of actinides at t=o to the total heat rate in core at t=o and is given as input data based on the following equation,

$$S^{ACT}(o) = \frac{C\ \Sigma_a}{Y\ \Sigma_f}(y + y') \tag{15}$$

where C and Σ_a stands for the conversion ratio and the effective neutron absorption cross section of U^{238} respectively and Σ_f represents the neutron fission cross section of U^{235} and y, y' and Y are the energy emissions due to a decay of U^{239}, a decay of $N_p{}^{239}$ and a fission of U^{235}. The ratio of heat generation rate from fission is given by interpolation of time dependent input data which are given as the ratio of fission heat at a time t to

that at the steady state, and by normalization as follows:

$$S^{FIS}(o) = 1 - S^{FP}(o) - S^{ACT}(o) \tag{16}$$

Table 1 Coefficients in the Shures equation

[Original]

time interval	A	a
$10^{-1} \leqq t < 10^{1}$	0.0603	0.0639
$10^{-1} \leqq t \leqq 1.5\times10^{2}$	0.0766	0.1807
$1.5\times10^{2} < t < 4\times10^{6}$	0.1301	0.2834
$4\times10^{6} \leqq t \leqq 2\times10^{8}$	0.2659	0.3350

[Modification]

time interval	A	a
$0 \leqq t < 0.1$	0.0699	0
$0.1 \leqq t < 7.76$	0.0603	0.0639
$7.76 \leqq t < 153.7$	0.0766	0.1807
$153.7 \leqq t < \infty$	0.1301	0.2834

Table 2 Heat Transfer Correlations in ASCOT-1

RELAP4-EM logic

Mode No.	Heat transfer regime	Correlation	Ref.
1	Subcooled forced convection	Dittus-Boelter	10
2	Nucleate boiling	Thom	11
3	Forced convection vaporization	Schrock-Grossman	12
4	Transition boiling	Mcdonough, Milich and King	13
5	Stable film boiling	Groeneveld 5.7	14
6	Pool film boiling	Berenson	15
7	Transition pool boiling		
8	Superheated vapor forced convection	Dittus-Boelter	10
9	Low pressure flow film boiling	Dougall-Rohsenow	16

HYDY-B1 logic

Mode No.	Heat transfer regime	Correlation	Ref.
1	Subcooled convective cooling	Dittus-Boelter	10
2	Nucleate boiling	Jens & Lottes	17
3	Stable film boiling	Groeneveld	14
4	Superheated steam convective cooling	McEligot et al.	18

2.3 Heat Transfer Coefficients

The heat conduction inside fuel rods and the energy conservation equation are coupled by the heat flux at the interface between the clad and the coolant. In ASCOT-1, two sets of heat transfer models are incorporated in order to determine the heat transfer coefficients; the RELAP4-EM heat transfer correlation selection logic[6] and the HYDY-B1[7] heat transfer correlation selection logic where nine and four heat transfer modes are provided respectively as shown in Table 2. In compliance with the requirements of Reference (8), after the critical heat flux is first predicted at an axial fuel rod location during blowdown, the nucleate boiling heat transfer correlation is not used at that location subsequently during the blowdown even if the calculated local fluid and surface conditions would apparently justify the re-establishment of nucleate boiling. The shift of the heat transfer mode from either nucleate boiling or forced convection vaporization to either transition boiling or stable film boiling is determined by the RELAP4-EM CHF correlation selection logic[6] or the GE transient CHF correlation[9] as shown in Table 3.

Table 3 Critical Heat Flux Correlations in ASCOT-1

Mode No.	Correlation	Reference
1	Babcock & Wilcox Company, B & W-2	19
2	Barnett	20
3	Modified Barnett	21
HYDY-B1 logic		
4	GE transient CHF correlation	9

3. Method of Computation

3.1 Two-dimensional Hydraulics of Core Flow

In the application of the set of bicharacteristic curve and compatibility conditions (5) through (9) to the numerical computation in a difference form, the method of variable mesh-spacing both in space coordinates and in time coordinate is used in the first-order accuracy calculation.[3]

The coolant pressure, velocity, density, sonic velocity, flow resistance, h_ρ and heating rate are known functions of (r,z) at a time t=T, given either from the initial condition or as a result of the calculation one stage in advance. These value at time T+ΔT are then to be determined (Fig. 1). Time mesh-spacing ΔT is determined by eq. (17).

$$\Delta T = \min_{r,z} \{1/(\frac{c+|v_r|}{\Delta r} + \frac{c+|v_z|}{\Delta z})\} \tag{17}$$

This means that the time increment must be such as to force the domain of dependence of the differential equations into the domain of dependence of the difference equations, to describe the difference equation only by adjacent mesh points, and to assure the stability of the difference equations.

In a three-variable case (two-space dimensional problems), the compatibility conditions involve the differentiation in two directions and there exist infinite characteristics and one particle line characteristic.

Eliminating the terms involving the spatial derivatives in Eq. (7), the basic equations are reduced to numerical integration along the four bicharacteristics and one path line characteristic. The bicharacteristics corresponding to $\theta=0$, $\frac{\pi}{2}$, π and $\frac{3}{2}\pi$ are selected here and are written as

$$\rho c \frac{D_0 v_r}{Dt} + \frac{D_0 p}{Dt} + \rho c^2 \frac{\partial v_z}{\partial z} = -c^2 \frac{\rho v_r}{r} - cF_r - \frac{(Q''' + Fe)c^2}{\rho h_\rho} \tag{18}$$

$$\rho c \frac{D_{\frac{\pi}{2}} v_z}{Dt} + \frac{D_{\frac{\pi}{2}} p}{Dt} + \rho c^2 \frac{\partial v_r}{\partial r} = -c^2 \frac{\rho v_r}{r} - c(F_z + \rho g_z) - \frac{(Q''' + Fe)c^2}{\rho h_\rho} \tag{19}$$

$$-\rho c \frac{D_{\pi} v_r}{Dt} + \frac{D_{\pi} p}{Dt} + \rho c^2 \frac{\partial v_z}{\partial z} = -c^2 \frac{\rho v_r}{r} + cF_r - \frac{(Q''' + Fe)c^2}{\rho h_\rho} \tag{20}$$

$$-\rho c \frac{D_{\frac{3\pi}{2}} v_z}{Dt} + \frac{D_{\frac{3\pi}{2}} p}{Dt} + \rho c^2 \frac{\partial v_r}{\partial r} = -c^2 \frac{\rho v_r}{r} + c(F_z + \rho g_z) - \frac{(Q''' + Fe)c^2}{\rho h_\rho} \tag{21}$$

where the subscripts of the operators D show θ's corresponding to the bicharacteristics. Substituting now Eq.(1) into Eq. (4), we obtain

$$\frac{Dp}{Dt} + \rho c^2 \left(\frac{\partial v_r}{\partial r} + \frac{\partial v_z}{\partial z}\right) + c^2 \frac{\rho v_r}{r} + \frac{(Q''' + Fe)c^2}{\rho h_\rho} = 0 \tag{22}$$

where $\frac{D}{Dt} = \frac{\partial}{\partial t} + vr \frac{\partial}{\partial r} + vz \frac{\partial}{\partial z}$. Eliminating the terms involving the spatial derivatives in Eqs. (18)∿(20), we obtain

$$\rho c \left[\frac{D_0 v_r}{Dt} + \frac{D_{\pi} v_r}{Dt} \right] + \left[\frac{D_0 p}{Dt} - \frac{D_{\pi} p}{Dt} \right] = -2cF_r, \tag{23}$$

$$\rho c \left[\frac{D_{\frac{\pi}{2}} v_z}{Dt} + \frac{D_{\frac{3\pi}{2}} v_z}{Dt} \right] + \left[\frac{D_{\frac{\pi}{2}} p}{Dt} - \frac{D_{\frac{3\pi}{2}} p}{Dt} \right] = -2c(F_z + \rho g_z), \tag{24}$$

$$\rho c \left[\frac{D_0 v_r}{Dt} - \frac{D_{\pi} v_r}{Dt} + \frac{D_{\frac{\pi}{2}} v_z}{Dt} - \frac{D_{\frac{3\pi}{2}} v_z}{Dt} \right] + \frac{D_0 p}{Dt} + \frac{D_{\frac{\pi}{2}} p}{Dt} + \frac{D_{\pi} p}{Dt} + \frac{D_{\frac{3\pi}{2}} p}{Dt}$$

$$-2 \frac{D_p p}{Dt} = -2c^2 \frac{\rho v_r}{r} - 2 \frac{(Q''' + Fe)c^2}{\rho h_\rho} \tag{25}$$

The finite difference approximation to the characteristic directions and the compatibility conditions can now be obtained by specifying the

planes of a constant time. The four bicharacteristics, $\theta=0$, $\theta=\frac{\pi}{2}$, $\theta=\pi$ and $\theta=\frac{3}{2}\pi$, and the particle line characteristic drawn back from each mesh point of the plane $t=T+\Delta T$ to the plane $t=T$ intersect with the plane $t=T$ at the points P1, P2, P3, P4 and P5, respectively (see Fig. 1). Values of the variables at each mesh point are calculated by linear interpolation of values known from the preceding calculations or the initial conditions. Finite difference approximation to Eqs. (23) ∿ (25) and (6) are thus obtained from the following explicit formula:

$$(\rho c)_0\left(v_r - \frac{v_r^1 + v_r^3}{2}\right) - \frac{p^1-p^3}{2} = -(cF_r)_0\Delta T \tag{26}$$

$$(\rho c)_0\left(v_z - \frac{v_z^2 + v_z^4}{2}\right) - \frac{p^2-p^4}{2} = -[c(F_z + \rho g_z)]_0\Delta T \tag{27}$$

$$(\rho c)_0(v_r^3 - v_r^1 + v_z^4 - v_z^2) + 2p - (p^1 + p^2 + p^3 + p^4) + 2p^5$$

$$= -2\left(c^2\frac{\rho v_r}{r} + \frac{(Q'''+Fe)c^2}{\rho h_\rho}\right)_0\Delta T \tag{28}$$

$$-(c^2)_0(\rho - \rho_5) + (p - p_5) = -\left(\frac{(Q'''+Fe)c^2}{\rho h_\rho}\right)_0\Delta T \tag{29}$$

where the superscripts represent the point number at $t=T$ as shown in Fig. 1. The subscript 0 indicates the value at $t=T$ and the variables without the subscripts or the superscripts refer to the values at $t=T+\Delta T$.

The order of the computation is as follows:

(1) Calculate the values with superscript in Eq. (26) through (29) by bilinear interpolations between mesh points,

(2) determine P at $t=T+\Delta T$ from Eq. (28),

(3) determine v_r, v_z and ρ from Eqs. (26), (27) and (29), respectively,

(4) determine c, Q''', h_ρ, Fr, Fz from a steam table or other equations,

(5) determine ΔT and a new T from Eq. (17),

(6) return to (1).

3.2 Heat Conduction inside Fuel Rods

The heat conduction process occurring inside the fuel rods is assumed to be one-dimensional: only radial conduction is allowed but axial and azimuthal conduction are ignored. The fuel pellet is subdivided into an assigned number of annular nodes of equal thickness and the fuel cladding is not subdivided and has only one node (Fig. 2).

By applying a first-order explicit formula to Eq. (10), temperature of each node at a time $T+\Delta T$ is given as follows:

$$Tn(T+\Delta T) = Tn(T) + \{Q_n(T) + q_n^{IN} - q_n^{OUT}\}\Delta T/Cn \tag{30}$$

where Tn stands for the temperature of the n-th node and

$$Cn = \begin{cases} C_p(Tn)\rho_p \pi \Delta r^2 (2n-1)\Delta Z & (n=1,2,..,N) \\ C_c(Tn)\rho_c \pi (r_{cos}^2 - r_{cis}^2)\Delta Z & (n=N1) \end{cases} \tag{31}$$

$$q_n^{IN} = \begin{cases} 0 & (n=1) \\ (T_{n-1}-T_n)/R_{n-1,n} = q_n^{OUT} & (n=2,3,\ldots,N) \\ q^{GAP} + Q_{CIS}^{MWR}, & (n=N_1) \end{cases} \tag{32}$$

$$q_n^{OUT} = \begin{cases} (T_n - T_{n+1})/R_{n,n+1} & (n=1,2,\ldots,N-1) \\ q^{GAP} & (n=N) \\ q^{CONV} - Q_{COS}^{MWR}, & (n=N_1) \end{cases} \tag{33}$$

where Q_{CIS}^{MWR} and Q_{COS}^{MWR} stand for heat generation due to the metal-water reaction on the outer and the inner surface of cladding, respectively, which are described in § 3.3,

$$Q_n \equiv \dot{Q}(T,n,i,j) = \dot{Q}^{CORE}(T)\cdot\Phi_{n,i,j}\cdot\Delta z_j \tag{34}$$

where

$$\Phi_{n,i,j} = \Delta Z_j \cdot S_i^{ROD}(T)\cdot S_j^{NODE}(T)\cdot S_n^{NODE}(T) \tag{35}$$

ΔZ_j : the mesh width of the j-th vertical node

S_i^{ROD} : the ratio of linear heat rate in a fuel rod belonging to the i-th concentric annular subregion to the total linear heat rate in a core

S_j^{NODE} : the ratio of linear heat rate in the j-th vertical node to the total linear heat rate in a fuel

S_n^{NODE} : the ratio of linear heat rate in the n-th radial node to the total linear heat rate inside a fuel.

In the above Eq's (30) through (34) are omitted the subscripts (i,j), which stand for belonging to the j-th vertical node within the i-th concentric annular subregion, for abbreviation. In Eq's (32) and (33), the thermal registances $R_{x,y}$'s are calculated as follows:

$$R_{n,n+1} = \frac{1}{2\pi\Delta Z}\frac{\Delta r}{r_n + r_{n+1}}/K_p\left(\frac{T_n + T_{n+1}}{2}\right)$$

$$R_{N,ps} = \frac{1}{2\pi\Delta Z}\frac{r_{ps} - r_N}{r_{ps} + r_N}/K_p(T_N)$$

$$R_{ps,CIS} = \frac{1}{2\pi\Delta Z}\frac{1}{r_{ps}}\frac{1}{h_{GAP}}$$

$$R_{CIS,N1} = \frac{1}{2\pi\Delta Z} \frac{r_{N1} - r_{CIS}}{r_{N1} + r_{CIS}} / K_p(T_{N1})$$

$$R_{N1,COS} = \frac{1}{2\pi\Delta Z} \frac{r_{COS} - r_{N1}}{r_{COS} + r_{N1}} / K_p(T_{N1})$$

and

$$R_{COS,BULK} = \frac{1}{2\pi\Delta Z} \cdot \frac{1}{r_{COS}} \cdot \frac{1}{h_{CONV}}$$

where r_x stands for the radius at the point X and h_{GAP} represents the gap conductance which is determined by selecting one of two input data according to whether there occurs the cladding deformation or not. The quantity h_{CONV} stands for the heat transfer coefficient which is given in Section 2.3. The quantities q^{GAP} and q^{CONV} are calculated with the following equations:

$$q^{GAP} = \frac{T_N - T_{N1} - Q^{MWR}_{CIS} R_{CIS,N1}}{R_{N,ps} + R_{ps,CIS} + R_{CIS,N1}} \tag{35}$$

and

$$q^{CONV} = \frac{T_{COS} - T_{BULK}}{R_{COS,BULK}} \tag{36}$$

The pellet surface temperature T_{ps} and the cladding inner and outer surface temperature, T_{CIS} and T_{COS} are determined as follows:

$$T_{ps} = T_N - q^{GAP} \cdot R_{N,ps} \tag{37}$$

$$T_{CIS} = T_{N1} + (q^{GAP} + Q^{MWR}_{CIS}) \tag{38}$$

$$T_{COS} = T_{BULK} + q^{CONV} R_{COS,BULK} \tag{39}$$

In ASCOT-1, the effect of the gamma smearing on the heat generation distribution may also be considered as follows:

$$S_i^{ROD}(T) = \gamma(T) S_i^{ROD,\gamma} + [1-\gamma(T)] S_i^{ROD,\bar{\gamma}}$$

$$S_j^{NODE}(T) = \gamma(T) S_j^{NODE,\gamma} + [1-\gamma(T)] S_j^{NODE,\bar{\gamma}}$$

$$S_n^{NODE}(T) = \gamma(T) S_n^{NODE,\gamma} + [1-\gamma(T)] S_n^{NODE,\bar{\gamma}}$$

$$\gamma(T) = [S^{FP}(T)\gamma^{FP} + S_{(T)}^{ACT}\gamma^{ACT} + S_{(T)}^{FIS}\gamma^{FIS}]/[S^{FP}(T) + S^{ACT}(T) + S^{FIS}(T)]$$

where

γ : contribution of the gamma ray absorption heating to the total heat generation in the core

γ^{FP}, γ^{ACT}, γ^{FIS} : contribution of the gamma ray absorption heating for the fission product, the actinide decay heat and for the fission heat respectively.

$S_i^{ROD,\gamma}$: gamma heat generation rate of the i-th concentric annular subregion in a fuel rod, relative to the total gamma heat generation rate in a core

$S_i^{ROD,\bar{\gamma}}$: non-gamma heat generation rate of the i-th concentric annular subregion in a fuel rod, relative to the total non-gamma heat generation rate in a core.

$S_j^{NODE,\gamma}$: gamma heat generation rate of the j-th vertical node, relative to the total gamma heat generation rate in a fuel rod

$S_j^{NODE,\bar{\gamma}}$: non-gamma heat generation rate of the j-th vertical node, relative to the total non-gamma heat generation rate in a fuel rod.

$S_n^{NODE,\gamma}$: gamma heat generation rate of the n-th radial node, relative to the total gamma heat generation rate inside a fuel

$S_n^{NODE,\bar{\gamma}}$: non-gamma heat generation rate of the n-th radial node, relative to the total non-gamma heat generation rate inside a fuel.

Therefore, the quantities $\Phi_{n,i,j}$, the space distribution function of heat generation, are modified as follows:

$$\Phi_{n,i,j} = \gamma(T) S_i^{ROD,\gamma} \cdot S_j^{NODE,\gamma} \cdot S_n^{NODE,\gamma}$$

$$+[1 - \gamma(T)] S_i^{ROD,\bar{\gamma}} \cdot S_j^{NODE,\bar{\gamma}} \cdot S_n^{NODE,\bar{\gamma}} \quad .$$

The quantities $S_i^{ROD,\gamma}$, $S_i^{ROD,\bar{\gamma}}$, $S_j^{NODE,\gamma}$, $S_j^{NODE,\bar{\gamma}}$, $S_n^{NODE,\gamma}$ and $S_n^{NODE,\bar{\gamma}}$ are given by input data or the following built-in data:

$$S_i^{ROD,\gamma} = W_{ROD}/W_{CORE}$$

$$S_i^{ROD,\bar{\gamma}} = 1/N_{ROD}$$

$$S_j^{NODE,\gamma} = W_j^{NODE}/W_{ROD}$$

$$S_j^{NODE,\bar{\gamma}} = \Delta Z_j/Z_{CORE}$$

$$S_n^{NODE,\gamma} = W_n^{NODE}/W_{ROD}$$

$$S_n^{NODE,\bar{\gamma}} = W_n^{NODE}/W_p$$

where

W_{ROD} : weight of a fuel rod

W_{CORE} : weight of a core

W_j^{NODE} : weight of the j-th axial node

W_n^{NODE} : weight of the n-th radial node inside a fuel rod

W_p : weight of a pellet

N_{ROD} : number of rods

3.3 Metal-Water Reaction

When zircaly is exposed at an elevated temperature to a steam atmosphere, an exothermic reaction becomes significant. As the cladding temperature rises the reaction becomes more violent. According to the requirement of Ref. (8), this reaction rate is calculated by the Bake-Just equation[10] described in terms of a parabolic rate law:

$$\frac{d\theta}{dt} = \frac{33.3}{\theta \rho_c^2} \exp\left(\frac{-22900}{T+273.15}\right) \tag{40}$$

where

θ : thickness of the oxide (cm)

ρ_c : density of the cladding (gr/cm^3)

T : temperature at the reacting metal-oxide interface (°C)

Integration of Equation (40) over a time step on the outer surface gives

$$(\theta_{COS})_{i+1} = \left[(\theta_{COS})_i^2 + 2 \cdot \alpha_{COS}^{MWR} \cdot \Delta t \cdot \frac{33.3}{\rho_c^2} \times \exp\left\{\frac{-22900}{(T_{COS})_i + 275.15}\right\}\right]^{\frac{1}{2}} \tag{41}$$

where the subscript COS stands for the outer surface of the cladding and α_{COS}^{MWR} represents a modification factor of the reaction rate which is given as input data. The subscripts i and i+1 show the time step numbers. The temperature T_{COS} is calculated by Eq.(39). When the cladding is calculated

to deform, the oxide thcikness on the outer surface is modified by the next equation (42) and is thereafter determined with Eq.(41),

$$(\theta_{COS})_{NEW} = \alpha^{REMAIN} \cdot \frac{(\theta_{COS})_{OLD}}{\alpha_{SWELL}} \tag{42}$$

where the subscripts OLD and NEW stand for before and after the deformation, respectively and α^{SWELL} represents the ratio of the diametral change before and after deformation and is given as input data. The quantity α^{SWELL} represents a parameter, to which 1 or 0 is given as input data depending on whether the oxide stretches like elastic or comes off during deformation.

The thickness of the oxide layer on the inner surface is calculated in the same way as on the outer surface as follows:

$$\theta_{CIS}\ (T+\Delta T) = \left[(\theta_{CIS})^2 + 2\cdot\alpha_{CIS}^{MWR}\cdot\Delta T\cdot\frac{33.3}{\rho_c^2}\cdot\exp\left\{\frac{-22900}{T_{CIS}(T) + 273.15}\right\}\right]^{\frac{1}{2}} \tag{43}$$

where the subscript CIS stands for the inner surface of the cladding and α_{CIS}^{MWR} represents a modification factor of the reaction rate which is given as input data. But θ_{CIS} is assigned to zero before deformation.

The correlation (40) is based on the assumption that an unlimited supply of steam exists for the reaction. If the reaction is sufficiently violent or the steam flow rate sufficiently low, the steam could possibly be consumed by the reaction. However, Ref. (8) requests an infinite steam supply even if the above situation is true, hence the code always assumes Eq. (40) to hold.

The heat of reaction is approximately 1.54×10^3 cal per gram of zirconium reacted. Therefore,

$$Q_{COS}^{MWR} = 1.54\times10^3 \cdot a_{COS}\{(\theta_{COS})_{i+1} - (\theta_{COS})_i\}\rho_c \tag{44}$$

$$Q_{CIS}^{MWR} = 1.54\times10^{3} \cdot a_{CIS}\{(\theta_{CIS})_{i+1} - (\theta_{CIS})_{i}\}\rho_{c} \quad (45)$$

where the quantities a_{COS} and a_{CIS} represent the outer surface area and the inner surface area of the cladding shown in § 3.4.

3.4 Clad Swelling and Rupture Model

In the present version, the fuel cladding tube is assumed to swell and rupture just after the clad temperature exceeds the burst temperature which is given as input data. After deformation, the diametral swelling is calculated from the following equation:

$$r_{COS}^{NEW} = r_{COS}^{OLD} \cdot \alpha^{SWELL} \quad (46)$$

$$\theta_{C}^{NEW} = \theta_{C}^{OLD}/\alpha^{SWELL} \quad (47)$$

$$r_{CIS}^{NEW} = r_{COS}^{NEW} - \theta^{NEW} \quad (48)$$

$$a_{COS}^{NEW} = 2\pi r_{COS}^{NEW}\Delta Z \quad (49)$$

$$a_{CIS}^{NEW} = 2\pi r_{CIS}^{NEW}\Delta Z \quad (50)$$

where the quantities r, θ and a represent radius, thickness and surface area, respectively, and the subscripts COS and CIS stands for the cladding inner and outer surface, respectively, the superscripts NEW and OLD mean after and before defromation, respectively. The quantities α^{SWELL} stands for the expansion ratio of the cladding radius when the deformation occurs.

3.5 Flow Resistance

The core region is treated as a continuous flow field and the flow resistance effect of the complicated flow boundary formed by fuel rods, control rods, spacers, grids, and other structures are represented by effective flow resistance of the form

$$F_z = F_z^{bundle} + F_z^{other} \tag{51}$$

and $$F_r = F_r^{bundle} + F_r^{other} \tag{52}$$

where

(1) for subcooled water or superheated steam

(1-1) $$F_z^{bundle} = \frac{4\lambda}{D_e} \frac{\rho v_z |v_z|}{2g_c} \tag{53}$$

(1-2) $$F_z^{other} = K_z \frac{\rho v_z |v_z|}{2g_c} \tag{54}$$

where $$\lambda = \begin{cases} 0.316\ R_e^{-0.25} & (3000 < R_e < 100000) \\ 64/R_e & (R_e \leq 3000) \end{cases}$$

$R_e = vD_e/\nu$

$v = (v_r^2 + v_z^2)^{1/2}$

D_e= hydraulic equivalent diameter of bundle

$K_z = K_z^r K_z^{fb}$

K_z^r : input; flow resistance coefficient before swelling or rupture

K_z^{fb} : input; change ratio of flow resistance coefficient due to swelling or rupture
or $1/(1-B)^2$

$$B = \frac{A_U - A_B}{A_U} \quad : \text{fractional blockage}$$

A_U : undeformed flow area

A_B : deformed flow area

(1-3) $$F_r^{bundle} = C^{bundle} \frac{4\lambda}{D_e} \frac{\rho v_r |v_r|}{2g_c} \tag{55}$$

(1-4) $$F_r^{other} = C^{other} K_z \frac{\rho v_r |v_r|}{2g_c} \tag{56}$$

where C^{bundle}, C^{other} : input

(2) for two-phase flow

(2-1) $$F_z^{bundle} = \frac{4\lambda_{sw}}{D_e} \frac{\rho_{sw} v_z |v_z|}{2g_c} \bar{R} \tag{57}$$

where SW : saturated water

$\bar{R}$: two-phase multiplier

$P<17.5775$ kg/cm^2 → Maltinelli-Nelson[24]

$P>17.5775$ kg/cm^2 → Thom[25]

(2-2) F_z^{other} : same as (1-2)

(2-3) $$F_r^{bundle} = \bar{R} \frac{4\lambda_{sw}}{D_e} \frac{\rho_{sw} v_r |v_r|}{2g_c} \tag{58}$$

(2-4) F_r^{other} : same as (1-4)

3.6 Boundary Conditions

Figure 3 illustrates the currently available boundary conditions for the bottom, right, top and left edges of the computing area, as specified by the input data for each particular problem. The left boundary is the axis of cylindrical symmetry or the rigid surface, the right boundary is the rigid wall and, the top and bottom boundary are the outflow or inflow.

As Fig. 4 shows, in all instances, the number of the necessary boundary conditions is equal to the number of points outside of the computing area of the five points that the four bicharacteristics and the particle path line drawn back from each mesh point of the plane $t=T+\Delta T$, intersect with the plane $t=T$. The necessary boundary conditions are calculated by interpolating the input data.

(1) SYMMETRY or RIGID : A symmetric boundary and a rigid boundary represent an axis or plane of symmetry and a rigid wall, respectively and the assumption is made that $v_r^1 = -v_r^3$ and $P^1 = P^3$ in Eq. (26) and (28), hence they are simplified as follows:

$$v_r = 0 \tag{59}$$

$$(\rho c)_0[v_z^4 - v_z^2] + 2p - (2p^1 + p^2 + p^4) + 2p^5 = -2\left(\frac{(Q''' + Fe)c^2}{\rho h_\rho}\right)_0 \Delta T \tag{60}$$

(2) OUTFLOW : The outflow boundary conditions are allowed to vary with position and time. As Fig. 4 shows, the boundary conditions considered here are described in relation to the top boundary, the treatment being entirely analogous at the bottom boundary. In this case, one of four bicharacteristics and a particle path line drawn back from a top boundary mesh point intersects with the plane $t=T$ outside of the defined domain and hence either the pressure or the axial velocity specified at that boundary

position is referred as follows:

$$p = p^2 + \frac{p^1+p^3}{2} - p^5 - (\rho c)_0 (v_{z_{specified}} - v_z^2 - \frac{v_r^3 - v_r^1}{2})$$

$$- [c(F_z + \rho g_z) + c^2 \frac{\rho v_r}{r} + \frac{(Q''' + Fe)c^2}{\rho h_\rho}]_0 \Delta T \qquad (61)$$

or

$$v_z = v_z^2 - \frac{v_r^3 - v_r^1}{2} - \frac{1}{(\rho c)_0}\{p_{specified} - p^2 - \frac{p^1+p^3}{2} + p^5\}$$

$$- [c(F_z + \rho g_z) + c^2 \frac{\rho v_r}{r} + \frac{(Q''' + Fe)c^2}{\rho h_\rho}]_0 \Delta T \ . \qquad (62)$$

These two equations are obtained from Eq. (28) and (27) by eliminating the variables with the superscript 4.

At the bottom boundary, eliminating the variables with the superscript 2 from Eq. (27) and (28), we have

$$(\rho c)_0 (v_z - v_z^4 - \frac{v_r^3 - v_r^1}{2} - p + p^4 + \frac{p^1 + p^3}{2} - p$$

$$= - [c(F_z + \rho g_z) - c^2 \frac{\rho v_r}{r} - \frac{(Q''' + Fe)c^2}{\rho h_\rho}]_0 \Delta T \qquad (63)$$

and either the pressure or the axial velocity specified at that boundary position is referred to.

(3) INFLOW : The inflow boundary conditions are allowed to vary with position and time. As Fig. 4 shows, four of four bicharacteristics and a particle path drawn back from a top boundary mesh point intersects with the plane t=T outside of the defined domain and hence the pressure, the density and the axial velocity or the radial velocity specified at that boundary position are referred to as follows:

$$v_z = v_z^2 + \frac{1}{(\rho c)_0}\{p_{specified} - p^2) + (\rho c^2)_0 (\frac{\partial v_r}{\partial r})_{specified} \Delta T$$

$$+ [c^2 \frac{\rho v_r}{r} - c(F_z + \rho g_z) + \frac{(Q''' + Fe)c^2}{\rho h_\rho}]_0 \Delta T\} \quad (64)$$

or

$$v_r = v_{r_{left}} + \frac{\Delta r}{(\rho c^2)_0 \Delta T}\{(\rho c)_0 (v_{z_{specified}} - v_z^2)$$

$$- (p_{specified} - p^2) - [c^2 \frac{\rho v_r}{r} - c(F_z + \rho g_z) - \frac{(Q''' + Fe)c^2}{\rho h_\rho}]_0 \Delta T\} \quad (65)$$

where the subscript left shows the value at the left adjacent mesh point. The equation is obtained by the finite difference approximation of Eq. (21).

At the bottom boundary, the treatment is entirely analogous to that at the top boundary.

4. Comparison with an Analytical Solution

To demonstrate the performance of ASCOT-1, an example was calculated and is shown in this chapter.

This sample problem was made to demonstrate the hydrodynamic part of ASCOT-1 by the transient gas flow in a cylindrical region with uniform heating. The configuration is shown in Fig. 5 and the equation of state in terms of the velocity of sound was taken to be

$$c^2 = p/\rho \tag{67}$$

and the ratio of the heat generation to the isobaric expansion term was taken to be

$$Q'''/\rho^2 h_\rho = -1 \quad \sec^{-1} \tag{68}$$

Other conditions were

1. Initial Conditions

$$v_r^0 = 0$$

$$v_z^0 = 0$$

$$p^0 = 10.134 \ kg_m/m\cdot sec^2$$

$$\rho^0 = 6408 \ kg_m/m^3$$

2. Boundary Conditions

$$v_z(t,r,0) = 0$$

$$p\ (t,r,3) = 10.134 \ kg_m/m\cdot sec^2$$

$$v_r(t,0,z) = 0$$

$$v_r(t,1,z) = 0$$

To obtain the numerical solution of the above problem by ASCOT-1, the input data KRMAX and KZMAX were set to 0 and a subroutine was added to calculate Eqs.(67) and (68).

It is shown in Fig. 6 that the results are very close to the following analytical solution (69) obtained by the method of separation of variables,

$$p(t,r,z) = p_0 \, e^{y(t,z)} \tag{69}$$

where

$$y(t,z) = \frac{2aX}{C_0} \sum_{n=1}^{\infty} \frac{[1+(-1)^{n+1}][Y_0(x_0)J_0(x) - J_0(x_0)Y_0(x)]}{n^2\pi^2[Y_0(x_0)J_1(x_0) - Y_1(x_0)J_0(x_0)]} \tag{70}$$

$$x_0 = -\frac{2}{a}\frac{n\pi}{X} C_0$$

$$x = -\frac{2}{a}\frac{n\pi}{X} C_0 e^{-\frac{at}{2}}$$

$$a = -1 \text{ sec}^{-1}$$

$$X = 6\text{m}$$

Further verification studies of ASCOT-1 are being carried out with both the two-dimensional flow problem with flow restrictions, power distributions and so on and the one-dimensional analytical solution mentioned above. The results will be reported later, together with discussions on the effects of spatial mesh spacing, power distributions etc. and the numerical stability.

Acknowledgement

The authors would like to their appreciations to K. Abe of Reactor Safety Code Development Laboratory at JAERI for his offering the program SCORCH-B2 and to the members of Reactor Safety Code Development Laboratory at JAERI for their valuable discussions.

where

$$y(t,z) = \frac{2aX}{C_0} \sum_{n=1}^{\infty} \frac{[1+(-1)^{n+1}][Y_0(x_0)J_0(x) - J_0(x_0)Y_0(x)]}{n^2\pi^2[Y_0(x_0)J_1(x_0) - Y_1(x_0)J_0(x_0)]} \tag{70}$$

$$x_0 = -\frac{2}{a}\frac{n\pi}{X} C_0$$

$$x = -\frac{2}{a}\frac{n\pi}{X} C_0 e^{-\frac{at}{2}}$$

$$a = -1 \text{ sec}^{-1}$$

$$X = 6\text{m}$$

Further verification studies of ASCOT-1 are being carried out with both the two-dimensional flow problem with flow restrictions, power distributions and so on and the one-dimensional analytical solution mentioned above. The results will be reported later, together with discussions on the effects of spatial mesh spacing, power distributions etc. and the numerical stability.

Acknowledgement

The authors would like to their appreciations to K. Abe of Reactor Safety Code Development Laboratory at JAERI for his offering the program SCORCH-B2 and to the members of Reactor Safety Code Development Laboratory at JAERI for their valuable discussions.

Reference

[1] M. Akimoto et al.: "ALARM-P1 : A Computer Program for Pressurized Water Reactor Blowdown Analysis", JAERI-M (to be published).

[2] V.J. Esposito and A.C. Spencer: "Can Macro-Micro-Type Computation Schemes Be Reactor Engineering Tools?", Proceedings of the Topical Meeting on Water Reactor Safety, Salt Lake City, Utah, March, 1973.

[3] K. Kobayashi and K. Namatame: "The Method of Characteristics for Axi-Symmetric Two-Dimensional Flows", JAERI-M 5969, January, 1975.

[4] K. Shure: "Fission Product Decay Energy", WAPD-BT-24, 1961.

[5] K. Abe and K. Sato: "SCORCH-B2: Simulation Code of Reactor Core Heatup during LOCA (For BWR, Second-version)", JAERI-M 6678, July, 1976.

[6] Regulatory Staff-Technical Review, U.S. Atomic Energy Commision, "WREM: Water Reactor Evaluation Model", October, 1974.

[7] Y. Asahi: "HYDY-B1 CODE: Calculational Model for Core Thermo-Hydraulics During a Loss-of-Coolant Accident", JAERI-M 6539, April, 1976.

[8] Committee on Reactor Safety Examination, Japanese Atomic Energy Commission: "Safety Evaluation Guide Line for Emergency Core Cooling Systems of Light-Water-Cooled Nuclear Power Reactors", May, 1974, as revised April, 1975.

[9] B.C. Slifer and J.E. Hench: "Loss-of-Coolant Accident and Emergency Core Cooling Models for General Electric Boiling Water Reactors", NEDO-10329, General Electric Company, Equation C-32, April, 1971.

[10] M. Jacob.: "Heat Transfer", Vol. 1, New York, Wiley & Sons (1957).

[11] J.R.S. Thom et al.: "Boiling in Subcooled Water During Flow Up Heated Tubes or Annuli", Proc. Instn. Mech. Engrs., Vol. 180, Part 3C (1966), p226-246.

[12] V.E. Schrock and L.M. Grossman, "Forced Convection Boiling Studies",

Final Report on Forced Convection Vaporization Project, TID-14632 (1959).

[13] J.B. McDonough, W. Millich, E.C. King, "Partial Film Boiling With Water at 2000 psig in a Round Vertical Tube", MSA Research Corp., Technical Report 62 (1958).

[14] D.C. Groeneveld, "An Investigation of Heat Transfer in the Liquid Deficient Regime", AECL-3281 (Rev.) (December 1968, revised August 1969).

[15] P.J. Berenson, "Film-Boiling Heat Transfer from a Horizontal Surface", J. of Heat Transfer, Vol. 83 (August 1961).

[16] R.S. Dougall and W.M. Rohsenow, "Film Boiling on the Inside of Vertical Tube with Upward Flow of the Fluid at Low Qualities", MIT-TR-9079-26 (1963).

[17] W.H. Jens and Lottes: "Analysis of Heat Transfer, Burnout, Pressure Drop and Density Data for High-Pressure Water", ANL-4627 (1951).

[18] D.M. McEligot, L.W. Ormand and H.C. Perkins, Jr., Trans. Amer. Soc. Mech. Engrs., 88, Series C, p.239-245, May, 1966.

[19] J.S. Gellerstedt et al.: "Correlation of Critical Heat Flux in a Bundle Cooled by Pressurized Water", pp63-71 of Two-Phase Flow and Heat Transfer in Rod Bundles, Symposium presented at the Winter Annual Meeting of the Amer. Soc. Mech. Engrs., Los Angeles, California (Nov. 1969).

[20] P.G. Barnett: "A Correlation of Burnout Data for Uniformly Heated Annuli and Its Use for Predicting Burnout in Uniformly Heated Rod Bundles", AEEW-R 463 (1966).

[21] E.D. Hughes: "An Examination of Rod Bundle Critical Heat Flux Data and Correlations and Their Applicability to Loss-of-Coolant Accident Analysises", Quarterly Technical Report Reactor Safety Program

Division, K.A. Dietz (ed.), ID-1319 (May 1970), pp16-40.

[22] L. Baker and L.C. Just: "Studies of Metal Water Reactions at High Temperaturesure, III. Experimental and Theoretical Studies of the Zirconium-Water Reaction", ANL-6548, May 1962.

[23] H. Blasius, Forsch. Arb. Ing. Wes., Nr. 131, (1924).

[24] R.C. Martinelli and D.B. Nelson: "Prediction of Pressure Drop during Forced Circulation Boiling of Water", Trans. ASME 70, 695-702 (1948).

[25] J.R.S. Thom, "Prediction of Pressure Drop during Forced Circulation Boiling Water", Int. J. Heat Mass Transfer, Vol. 7, pp.709-724, Pergamon Press 1964.

Appendix A Nomenclature

A	Flow area
B	Fractional blockage
c	Sonic velocity
C	Conversion ratio
c_p	Specific heat capacity
D/Dt	Derivative with respect to a characteristic direction
De	Hydraulic equivalent diameter
F	Flow resistance
Fe	Irreversible energy due to frictional losses
g	Gravitational acceleration
h	Enthalpy
h_ρ	$(\partial h/\partial \rho)P$
h_{CONV}	Convective heat transfer coefficient
h_{gap}	Gap conductance
k	Thermal conductivity
K	Flow resistance coefficient
P	Pressure
$\dot{Q}$	Heat generation rate in the (i,j)th subregion
Q'''	Heat generation rate per unit volume
r	Radius
R	Thermal resistance
$\bar{R}$	Two phase multiplier
S	Ratio of heat rate from a heat source to $\dot{Q}^{CORE}(0)$
T	Time
T	Temperature
v	Flow velocity

y	Energy emission due to a decay of U^{239}
y'	Energy emission due to a decay of Np^{239}
Y	Energy emission due to a decay of U^{235}

Greek symbols

α	Modification factor
Δ	Mesh width
θ	Angle
θ	Thickness of oxide
λ	Fanning friction factor
ν	Kinematic viscosity
ρ	Density
Σ_a	Effective neutron absorption cross section
Σ_f	Effective neutron fission cross section
Φ	Space-distribution function of heat generation

Subscripts

ACT	Decay of actinide
B	Deformed
c	Cladding
CIS	Cladding inner surface
COS	Cladding outer surface
FIS	Fission heat
FP	Fission product decay
p	Pellet
P	In partide path direction
r	In r-direction
SW	Saturated water
U	Undeformed

Z	In z-direction
θ	In bicharacteristic direction corresponding to θ

Superscripts

CORE	In core
fb	Flow blockage
MWR	Methal water reaction
r	Before swelling or rupture

Appendix B Input Data Description

1. REAG Input Routine

All input data are read into the ASCOT program in free format via a generalized subroutine REAG. Subroutine REAG for FACOM 230-75 converts BCD information to integer or floating point binary information; three conversion types, i.e. type of reading N floating numbers, type of reading N interger numbers and mixed type of reading $4*N_1$ characters, N_2 integers and N_3 floating point numbers, respectively, are allowed by corresponding subroutines.

To explain how to arrange the data, a typical example of the function of this subroutine is shown below suppose the following three punched cards:

105, 318, -14, 1.5E-3, 3.12E-3/THIS IS A COMMENT

2(1.0, 1.5), 3(0)/

1.0, 5*0.1, 2*-0.2/

The subroutine will convert BCD number 105 and 318 to their binary integer equivalents. In a similar fashion -14 will be converted to a negative binary integer, and 1.5E-3 will be converted 0.0015. Data punched on a card may be delimted by blank column or comma. The slash (/) indicates the end of the BCD field to be converted. If no slash is present, 72 colmns of a card are scanned and next card is read.

The second card indicates that the data words 1.0 and 1.5 in the first parentheses and 0 in the second are repeated twice and three times, respectively, and therefor it is equivalent with a card punched as

1.0, 1.5, 1.0, 1.5, 0, 0, 0/.

The last card indicates that the first word is 1.0, the second word 0.1 is successively accumulated to the previous word five times and the last word -0.2, twice. Therefore it is equivalent with a card punched as

1.0, 1.1, 1.2, 1.3, 1.4, 1.5, 1.3, 1.1/.

JAERI-M-4458 the user's guide of "The subroutine to read the data in free format" is referred to for more detailed information.

2. Input Data

An ASCOT1 problem consists of a title card, type number cards, and data cards. Each datum corresponds to a "card number" and a "type number" and it is necessary to provide the data according to the following rules:

(1) The data of the same "type number" must be ranged in the order specified in the next paragraph,

(2) The data corresponding to different " card number"s may not be on the same card.

Title Card

The first data of an ASCOT-1 problem must be alpha-numelic characters for title specification in Column 1-72.

Type No.1

Card No.1 1 (Type No.)

Card No.2 IRMAX, IZMAX, KRMAX, KZMAX, NMAX, IBZ, INCONR, INCONZ, NHTCOP: where,

IRMAX the number of mesh points in the radial direction,

IZMAX the number of mesh points in the axial direction,

KRMAX the number of mesh points for the calculation of heat transfer in the radial direction,

KZMAX the number of mesh points for the calculation of heat transfer in the axial direction,

NMAX the number of mesh points in the radial direction in a representative fuel rod,

IBZ the number of points on which the flow resistances in the

axial direction except for the rod bundles are given,

INCONR the number of mesh points in the radial direction on which initial values of initial conditions are given,

INCONZ the number of mesh points in the axial direction on which initial value of initial conditions are given,

NHTCOP Heat transfer coefficient index,
=0, if HYDY-B1 correlation set is selected,
=1, if RELAP-4 correlation set is selected,

Type No.2

Card No.1 2 (Type No.)

Card No.2 IOUT, IPOUT, IPLOT, INTVP, NOUT1, NOUT2, NREST, NDVRT: where,

IOUT Print control. Pressure, velocity, density, sonic velocity and clad temperature etc. are printed out on every IOUT plus one time steps,

IPOUT Print control. Pressure, velocity, density, sonic velocity and/or clad temperature etc. at IPOUT mesh points are printed out on every time step (see Type No.9)

IPLOT Output index
=1, if the print output only,
=2, if the print output and the plot output,

INTVP Time scaling index for plot output:
=1 for 0∿0.2 sec,
=2 for 0.2∿10 sec,
=3 for 10∿600 sec,
=4 for 600∿ sec,

NOUT1, NOUT2 Print control. Pressure, velocity, density, clad temperature etc. are printed out from the NOUT1-th to the NOUT2-th time step,

NREST File control for restarting,

=0 if no file used,

=N(>0) if store the information for restarting on the FORTRAN unit No. N,

=-N(<0) if restart with the file of the FORTRAN unit No. N,

NDVRT Boundary condition index at r=0 and $r=R_{max}$,

=0 for $\partial/\partial r=0$,

=1 for Vr=0,

NDVTT 0 (Constant)

Type No.3

Card No.1 3 (Type No.)

Card No.2 ITER, EPS, TMAX: where,

ITER Upper limit of the iteration number of the initial condition calculation

EPS Convergence criteria of the initial condition calculation

TMAX Problem time span (sec)

Type No.4

Card No.1 4 (Type No.)

Card No.2 (R(I), I=1, IRMAX): where,

R The radial coordinates of mesh points, (m)

Card No.3 (Z(I), I=1, IZMAX): where,

Z The axial coordinates of mesh points, (m)

Card No.4 PZLOW, PZUP: where,

PZLOW The axial coordinates of the boundary between the lower plenum and the core, (m)

PZUP The axial coordinates of the boundary between the upper plenum

and the core,

Type No.5

Card No.1 5 (Type No.)

Card No.2 (NR(I), I=1, KRMAX): where,

NR The numbers of mesh points in the radial direction for the calculation of heat transfer,

Card No.3 (NZ(I), I=1, KZMAX): where,

NZ The numbers of mesh points in the axial direction for the calculation of heat transfer,

Type No.6

Card No.1 6 (Type No.)

Card No.2 RPELET, RCLADI, RCLADO, QCOREO: where,

RPELET Pellet radius (m)

RCLADI Inner radius of cladding (m)

RCLADO Outer radius of cladding (m)

QCOREO Initial total power (m)

Card No.3 (NFUEL(I), I=1, IRMAX-1): where,

NFUEL The number of fuel rods in each radial subregion,

Card No.4 (NCNTR(I), I=1, IRMAX-1): where,

NCNTR The number of control rods in each radial subregion,

Type No.7

Card No.1 7 (Type No.)

Card No.2 (ZB(I), I=1, IBZ): where,

ZB The axial coordinates of the planes on which the flow resistances except rod bundles, e.g. spacers and grids, exist, (m)

Card No.3 (CKZRSP(I), I=1, IBZ): where,

CKZRSP $=K_z^r$ The flow resistance coefficient before swelling or rupture at Z=ZB

Type No.8

Card No.1 8 (Type No.)

Card No.2 ((CF(I,J), I=IRMAX), J=1, IZMAX): where,

CF=c^{bundle} The ratio of the frictional pressure loss coefficient due to rod bundles in the radial direction to that in the axial direction

Card No.3 ((CB(I,J), I=IRMAX), J=1, IZMAX): where,

CB=c^{other} The ratio of the flow resistance coefficient due to any other obstructions than rod bundles in the radial direction to that in the axial direction

Card No.4 ((CKZR(I,J), I=IRMAX), J=1, IZMAX): where,

CKZR=K_z^r The flow resistance coefficient

Type No.9

Card No.1 9 (Type No.)

Card No.2 ((IROZOK(I,J), I=1,3), J=1, IPOUT): where,

IROZOK(1,J) The mesh point number in the radial direction of the J-th print out point,

IROZOK(2,J) The mesh point number in the axial direction of the J-th print out point,

IROZOK(3,J) Content index:

=1 for pressure only

=2 for radial velocity only

=3 for axial velocity only

=4 for temperature only

=5 for clad temperature only

=6 for all shown above

Type No.10

Card No.1 10 (Type No.)

Card No.2 (RIC(I), I=1, INCONR): where,

RIC The radial coordinates of the points where the initial conditions are given, (m)

Card No.3 (ZIC(I), I=1, INCONZ): where,

ZIC The axial coordinates of the points where the initial conditions are given. (m)

Type No.11

Card No.1 11 (Type No.)

Card No.2 ((PO(I,J), RHO(I,J), VRO(I,J), VZO(I,J), QO(I,J), TCLO(I,J), I=1, INCONR), J=1, INCONZ): where,

PO initial pressure ($kg_m/m \cdot sec^2$)

RHO initial density (kg_m/m^3)

VRO initial radial velocity (m/sec)

VZO initial axial velocity (m/sec)

QO initial heat generation rate ($kcal/m^3 \cdot sec$)

TCLO initial clad temperature (°C)

Type No.12

Card No.1 12 (Type No.)

Card No.2 NTABBK: where,

NTABBK The numbers of points of the flow blockage table

Card No.3 ((TABBK(I,J), I=1,2), J=1, NTABBK): where,

TABBK(1,J)=$B_j=(A_U-A_B)/A_U$: fractional blockage

TABBK(2,J)=K_z^{fb}: change ratio of flow resistance coefficient due to swelling or rupture

Type No.13

Card No.1 13 (Type No.)

Card No.2 NTABR, NTABT**, NBLIN*, NBLOU*, NBUIN*, NBUOU*: where,

NTABR The number of the radial mesh points where the boundary conditions are given,

NTABT The number of the time mesh points where the boundary conditions are given,

NBLIN Lower boundary condition index for inflow
=1 radial velocity
=2 axial velocity

NBLOU Lower boundary condition index for outflow
=1 pressure
=2 axial velocity

NBUIN Upper boundary condition index for inflow
=1 radial velocity
=2 axial velocity

NBUOU Upper boundary condition index for outflow
=1 pressure
=2 axial velocity

If NTABT>0, the boundary conditions are read in through the SYSIN file

---

* The number of the necessary boundary conditions at each boundary mesh point depends on which of inflow and outflow occurs there. In the case of the inflow, three boundary conditions are necessary, i.e. pressure, density and either radial velocity (NB*IN=1) or axial velocity (NB*IN=2). In the case of the outflow, one boundary condition is necessary, i.e. pressure (NB*OU=1) or axial velocity (NB*OU=2).

** The boundary conditions can be read in from the SYSIN file (card input) or from an outer memory unit. If the card input is selected, NTABT must be positive. If the outer memory unit is chosen, NTABT must be negative and the reference number of the outer memory unit is equal to |NTABT|.

(card input) as follows,

Card No.3 (TABR(I), I=1, NTABR): where,

TABR The radial coordinates of the mesh points where the boundary conditions are given. (m)

I=1∿NTABT

Card No.4 TABT(I): where,

TABT Time (sec)

Card No.5 (TABLPR(I,J), TABLRH(I,J), TABLVE(I,J), TABUPR(I,J), TABURH(I,J), TABUVE(I,J), J=1, NTABR): where,

TABLPR pressure
TABLRH density
TABLVE velocity
} at the J-th radial mesh point on the lower boundary,

TABUPR pressure
TABURH density
TABUVE velocity
} at the J-th radial mesh point on the upper boundary,

If NTABT<0, then the boundary conditions are read in from the outer memory unit, reference number of which is |NTABT|. The data format is assumed to be as follow:

```
READ(|NTABT|)   (TABR(I), I=1, NTABR)
DO 210 I=1,NTIMST
210 READ(|NTABT|)   TABT(I), (TABLPR(I,J), TABLRH(I,J), TABLVE(I,J),
        TABUPR(I,J), TABURH(I,J), TABUVE(I,J), J=1, NTABR)
```

where

NTIMST The number of time steps. It is necessary for the time at the NTIMST-th time step to be greater than the problem time span.

TABR, TABT, TAB*** double precision real variables

Type No.14

Card No.1 14 (Type No.)

Card No.2 NTDIM, LOGFIS: where,

NTDIM The number of the data points of the table of time vs. relative fission power

LOGFIS Interpolation index:

=0 linear interpolation of the data

=1 linear interpolation of the logarithm of the data

Card No.3 (TIM(I), I=1, NTDIM): where,

TIM time (sec)

Card No.4 (FIS(I), I=1, NTDIM): where,

FIS The ratio of the fission power at t=TIM(I) to that at t=0.

Type No.15*

Card No.1 15 (Type No.)

Card No.2 (NOTECP(I), I=1,5): where,

NOTECP Comment on the input data of the pellet heat capacity up to 20 characters,

Card No.3 INPCP: where,

INPCP The number of the data points of the table of temperature vs. heat capacity of pellet,

Card No.4 (TEM(I), I=1, INPCP): where,

TEM Temperature, (°C)

Card No.5 (CP(I), I=1, INPCP): where,

CP Heat capacity of pellet, (cal/gr °C)

Type No.16*

Card No.1 16 (Type No.)

Card No.2 (NOTECC(I), I=1,5): where,

NOTECC Comment on the input data of the cladding heat capacity up to 20 characters,

* If no input cards of this type number are given, the built-in correlation in used. (See Reference D).

Card No.3 INPCC: where,

INPCC The number of the data points of the table of temperature vs. heat capacity of cladding,

Card No.4 (TEM(I), I=1, INPCC): where,

TEM Temperature,

Card No.5 (AK(I), I=1, INPCC): where,

CC Heat capacity of cladding

Type No.17*

Card No.1 17 (Type No.)

Card No.2 (NOTELP(I), I=1,5): where,

NOTELP Comment on the input data of the pellet thermal conductivity up to 20 characters,

Card No.3 INPLP: where,

INPLP The number of the data points of the table of temperature vs. thermal conductivity of pellet,

Card No.4 (TEM(I), I=1, INPLP): where,

TEM Temperature (°C)

Card No.5 (AK(I), I=1, INPLP): where,

AK Thermal conductivity of pellet,

Type No.18*

Card No.1 18 (Type No.)

Card No.2 (NOTELC(I), I=1,5): where,

NOTELC Comment on the input data of the cladding thermal conductivity up to 20 characters,

Card No.3 INPLC: where,

INPLC The number of the data points of the table of temperature vs. cladding thermal conductivity,

Card No.4 (TEM(I), I=1, INPLC): where,

TEM Temperature

Card No.5 (AK(I), I=1, INPLC): where

AK Thermal conductivity of cladding

Type No.19*

Card No.1 19 (Type No.)

Card No.2 RHOP, RHOC: where,

RHOP Pellet density

RHOC Cladding density

Type No.20*

Card No.1 20 (Type No.)

Card No.2 INPGP: where,

INPGP The number of input data

Card No.3 (HTCGAP(I), I=1, INPGP): where,

HTCGAP(1) Gap conductance before deformation

HTCGAP(2) Gap conductance after deformation

(IF INPGP=1, HTCGAP(2)=HTCGAP(1)),

Type No.21

Card No.1 21 (Type No.)

Card No.2 SACTO, SFPMLT, SFISG, SACTG, SFPG: where,

SACTO=$S^{ACT}(0)$ Fraction of actinide decay heat to the total reactor power in steady state,

SFPMLT=α^{FP} The modification factor to the Shure's correlation (Eq.(13)),

SFISG Fraction of heat generation due to γ-ray absorption to the total fission power

SACTG Fraction of heat generation due to γ-ray absorption to the total actinide decay heat,

SFPG Fraction of heat generation due to γ-ray absorption to the total fission product decay heat,

Type No.22**

Card No.1 22 (Type No.)

Card No.2 (SKR(I), I=1, KZMAX): where,

$SKR=S_j^{NODE,\bar{\gamma}}$: relative heat generation in the j-th vertical node to the total one in a fuel, considering only the other nuclear reaction than the gamma heating

Type No.23**

Card No.1 23 (Type No.)

Card No.2 (SKG(I), I=1, KZMAX): where,

$SKG=S_j^{NODE,\gamma}$: relative heat generation in the j-th vertical node to the total one in a fuel, considering only the gamma heating

Type No. 24**

Card No.1 24 (Type No.)

Card No.2 (SMR(I), I=1, KRMAX): where,

$SMR=S_i^{ROD,\bar{\gamma}}$: relative heat generation in a fuel rod belonging to the i-th concentric annular subregion to the total one in a core, considering only the other nuclear reaction than the gamma heating

** If no input cards of this type number are given, the built-in data are used (See § 3.2).

Type No.25**

Card No.1 25 (Type No.)

Card No.2 (SMG(I), I=1, KRMAX): where,

$SMG=S_i^{ROD,\gamma}$: relative heat generation in a fuel rod belonging to the i-th concentric annular subregion to the total one in a core, considering only the gamma heating

Type No.26**

Card No.1 26 (Type No.)

Card No.2 (SNR(I), I=1, NMAX+1): where,

$SNR=S_n^{NODE,\bar{\gamma}}$: relative heat generation in the n-th radial node in a fuel rod to the total one in the fuel rod, considering only the other nucleate reaction than the gamma heating

Type No.27**

Card No.1 27 (Type No.)

Card No.2 (SNG(I), I=1, NMAX+1): where,

$SNG=S_n^{NODE,\gamma}$: relative heat generation in the n-th radial node in a fuel rod to the total one in the fuel rod, considering only the gamma heating

Type No.28

Card No.1 28 (Type No.)

Card No.2 (RBR(I), I=1, NMAX): where,

RBR Mesh width inside a fuel rod (m)

Type No.29

Card No.1 29 (Type No.)

Card No.2 ((DELW(I,J), I=1, IRMAX), J=1, NCZLW-1): where,

DELW Equivalent Diameters in the lower plenum (m)

Card No.3 ((DEUP(I,J), I=1, IRMAX), J=1, IZMAX-NCZUP): where,

DEUP Equivalent Diameters in the upper plenum (m)

B.2 Output Description

The first page of the output is a print of the input data. If there are any grammatical errors on the input data cards, the error message will be printed out here by the subroutine 'REAG' and the computer run will be terminated.

The information on the title card is printed out on the top of each page. The following quantities are printed out on every IOUT plus one time steps and from the NOUT1-th to the NOUT2-th time step:

pressure

velocity (radial and axial)

density

sonic velocity

clad surface temperature etc.

The specified quantities of those above mentioned are printed out on every time step.

Appendix C Steam Table for ASCOT-1

The SPADE computer program[1] generates tables of water properties and outputs these tables into a data set file in the proper format for ASCOT-1. The properties stored in the tables as functions of pressure and density include temperature, sonic velocity and $(\frac{\partial h}{\partial \rho})_p$. On the other hand, the IFC formulation for industrial use (1967)[2] have pressure and temperature or temperature and specific volume as the independent variables. Thus the main purpose of SPADE is to transform independent variables with the iterative scheme of linear interpotation and to generate the steam tables.

Appendix C Reference

1. K. Kobayashi and S. Sasaki, SPADE: A computer program for generating the steam tables having pressure and density as the independent variables (to be published).
2. JSME Steam Tables.

Appendix D Fuel Rods Material Properties built in ASCOT-1

D.1 Properties of Zircaloy-4

D.1.1 Heat Capacity[1]

$$C_c = \begin{cases} 6.84\times10^{-2}+2.39\times10^{-5}T\ [cal/gr°C] & (T<747) \\ 8.6\times10^{-2}\ [cal/gr°C] & (T\geqq747) \end{cases}$$

D.1.2 Thermal Conductivity[2]

$$K_c = 3.010\times10^{-5}T+0.02633\ [cal/cm\cdot sec°C]$$

D.1.3 Density[3]

$$\rho_c = 6.55\ [gr/cm^3]$$

D.2 Properties of Uranium Dioxide

D.2.1 Heat Capacity[4]

$$C_p = 0.0657-0.9556\times10^{-6}T+0.8123\times10^{-8}T^2\ [cal/gr°C)$$

D.2.2 Thermal Conductivity[5]

$$K_p = \frac{9.135}{402.4+T} + 1.463\times10^{-13}(T+273.0)^3\ [cal/cm\cdot sec°C]$$

D.2.3 Density[6]

$$\rho_p = 10.65\ [gr/cm^3]$$

D.3 Appendix D References

1. H.C. Brassfield, J.F. White, L. Sjodahl, J.T. Bittel, GEAP-482 (April 1968)
2. A. Morishima et al.: JAERI-M 4881, D-178 (⑦ WAPD-TM-652)
3. ibid., D-165
4. ibid., D-700 (⑦ JAERI-1235, EUREKA)
5. ibid., C-533 (⑳ GE '67 BWR)
6. ibid., D-524 (95% of Theoretical Density)

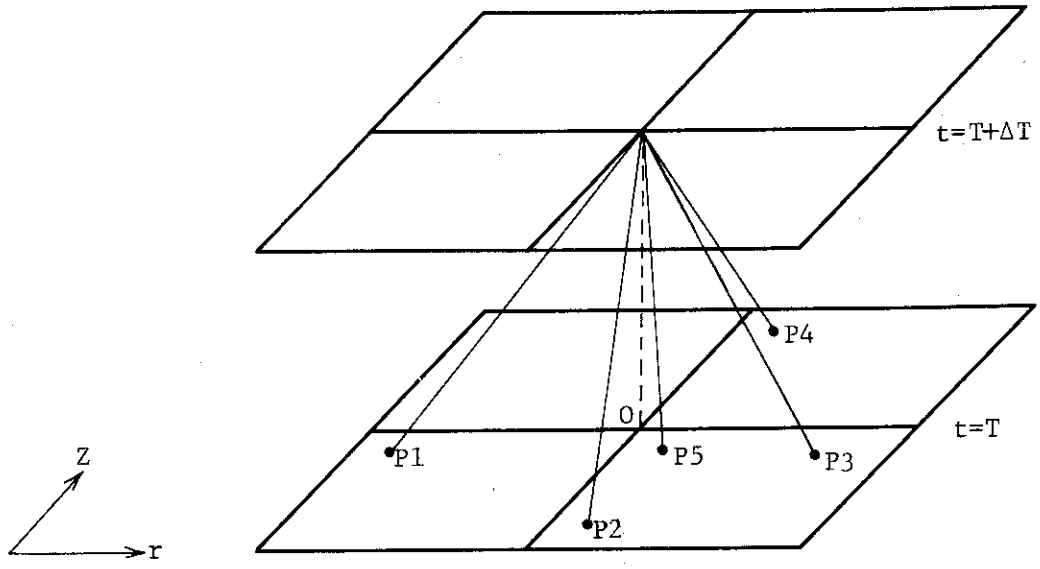

Fig. 1 Four bicharacteristics and particle path line from t=T+ΔT to t=T

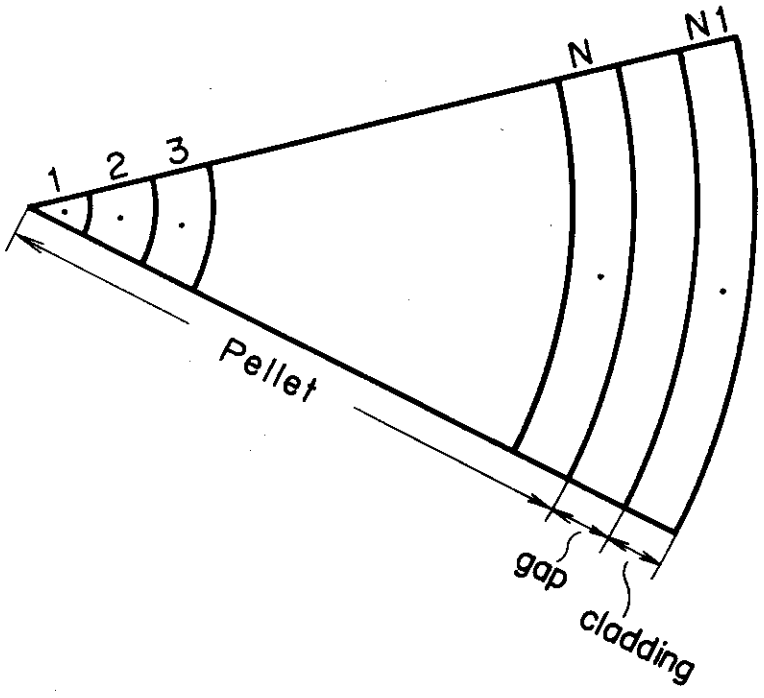

Fig. 2 Radial nodalization within the fuel Rod

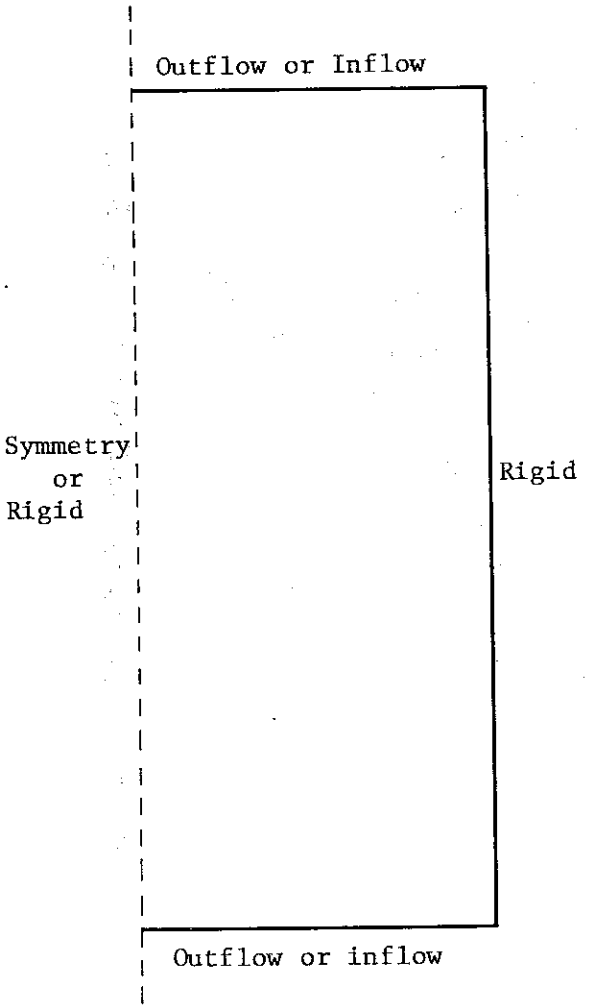

Fig. 3 Boundary conditions available in ASCOT

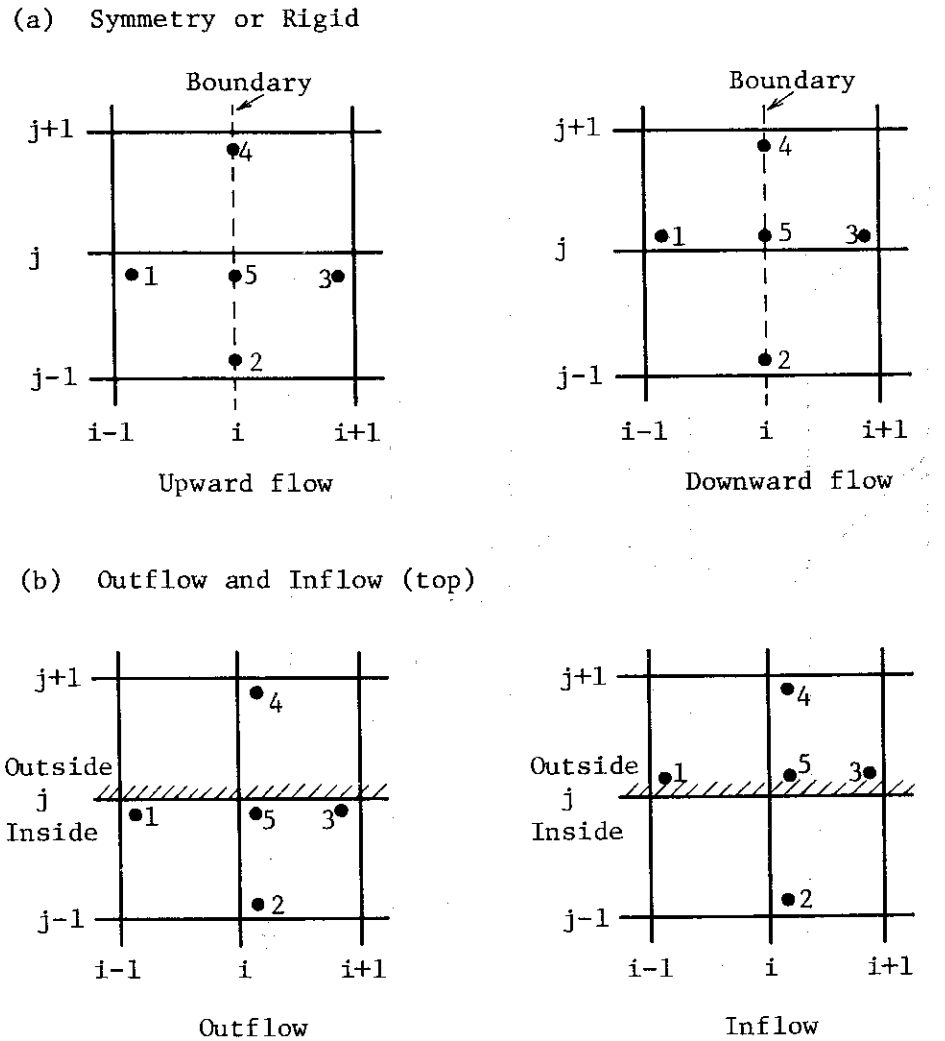

Fig. 4 Five points that four bicharacteristics and particle path line drawn back from (i,j) point of plane t=T+ΔT intersect with plane t=T

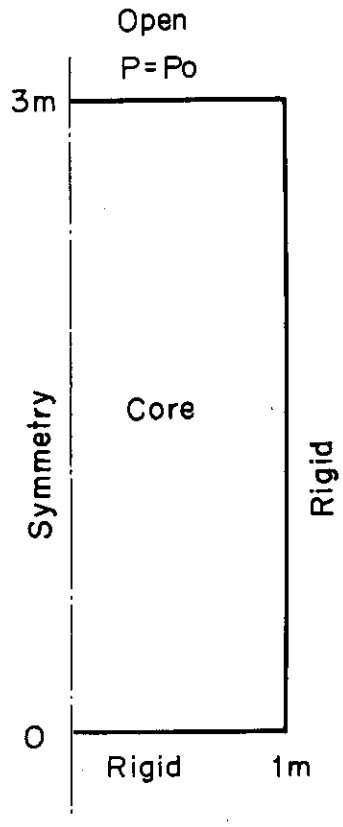

Fig. 5 A Core Configulation and Boundary Conditions for the transient gas flow with uniform heating.

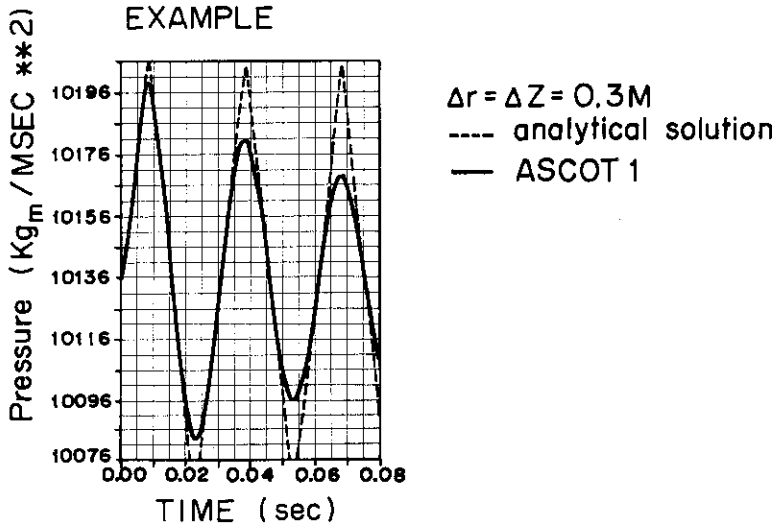

Fig. 6 Pressure at Closed End (Bottom)